

LaCo: Efficient Layer-wise Compression of Visual Tokens for Multimodal Large Language Models

Juntao Liu, Liqiang Niu, Wenchao Chen, Jie Zhou, Fandong Meng

Pattern Recognition Center, WeChat AI, Tencent Inc, China

{gentoliu, poetniu, cwctchen, withtomzhou, fandongmeng}@tencent.com

Abstract

Existing visual token compression methods for Multimodal Large Language Models (MLLMs) predominantly operate as post-encoder modules, limiting their potential for efficiency gains. To address this limitation, we propose LaCo (Layer-wise Visual Token Compression), a novel framework that enables effective token compression within the intermediate layers of the vision encoder. LaCo introduces two core components: 1) a layer-wise pixel-shuffle mechanism that systematically merges adjacent tokens through space-to-channel transformations, and 2) a residual learning architecture with non-parametric shortcuts that preserves critical visual information during compression. Extensive experiments indicate that our LaCo outperforms all existing methods when compressing tokens in the intermediate layers of the vision encoder, demonstrating superior effectiveness. In addition, compared to external compression, our method improves training efficiency beyond 20% and inference throughput over 15% while maintaining strong performance.

1 Introduction

Multimodal Large Language Models (MLLMs), such as LLaVA(Li et al., 2024a; Liu et al., 2023a, 2024, 2023b), InternVL(Chen et al., 2024e,d), and QwenVL(Bai et al., 2023; Wang et al., 2024b), have exhibited impressive capabilities in fusing visual and linguistic modalities. These models significantly enhance performance across a wide range of vision-language tasks, including visual question answering, image captioning, and beyond.

Typically, most MLLMs follow the LLaVA framework, in which visual inputs are first encoded into embeddings using a visual encoder and subsequently transformed into a representation compatible with the large language model (LLM) through a projector. The visual embeddings are then concatenated with textual inputs and processed jointly

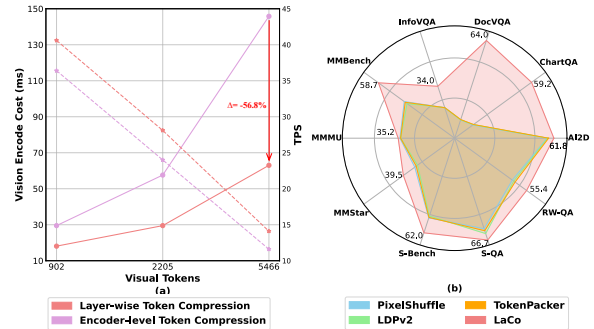


Figure 1: (a) The solid and the dotted represent vision encoding cost (VEC) and tokens per second (TPS), respectively. Layer-wise token compression improves the inference efficiency by 56.8% and 18.0% in terms of VEC and TPS. (b) LaCo outperforms other compression methods. All methods are implemented on AIMv2.

by an integrated LLM. In practice, the number of visual tokens can vary from hundreds to thousands, significantly increasing the running time of MLLMs. Recent studies (Shang et al., 2024; Ye et al., 2024; Chen et al., 2024b) have shown that the visual information processed by these models often contains a considerable degree of redundancy. As a result, visual token compression has emerged as a growing area of interest within multimodal learning research.

Previous approaches to visual token compression in multimodal models have mainly focused on external mechanisms applied after the visual encoder. For instance, InternVL utilizes pixel-shuffle(Shi et al., 2016) to merge adjacent tokens within a grid, while QwenVL applies a two-layer MLP to aggregate the neighboring tokens following the 32-layer ViT encoder. Gemma3(Kamath et al., 2025) adopts the average pooling technique to reduce the number of tokens generated by the SigLIP(Zhai et al., 2023) encoder. However, these methods fail to fully exploit the potential for improving efficiency in visual token compression, as they neglect the opportunities within the intermediate layers of the encoder itself.

In this study, we propose **LaCo**, a **L**ayer-wise token **C**ompression method that incorporates the pixel-shuffle and residual connection to effectively prune visual tokens. Specifically, our approach inserts a Patch Merge Layer (PML) after the k -th layer of the vision encoder to perform token compression. The PML utilizes pixel-shuffle to merge adjacent visual tokens and then employs a two-layer MLP to map the dimensionality of the merged tokens to the original size. In addition, to mitigate the information loss problem when compressing tokens, inspired by [Chen et al. \(2024a\)](#), we introduce an extra non-parametric shortcut to the PML to let the model learn residuals based on the space-to-channel operation. As a result, the proposed PML with residual connection can effectively compress visual tokens with almost no information loss.

We evaluate the effectiveness of our methods through extensive experiments, which are conducted following the guidance outlined by [Li et al. \(2024a\)](#). Our LaCo outperforms all existing methods when compressing tokens within the intermediate layers of the vision encoder across all scenarios. Compared to external compression, inner-layer compression with LaCo improves training and inference efficiency by over 20% and 15%, respectively, while maintaining strong performance. Furthermore, we conduct a comprehensive exploration of layer-wise token compression by placing LaCo at different depths of the encoder and applying vision encoders including AIMv2([Fini et al., 2024](#)), SigLIP([Zhai et al., 2023](#)), and InternViT([Chen et al., 2024e](#)), demonstrating the flexibility and generalizability of our method.

Our contributions are summarized as follows:

- We propose **LaCo**, a layer-wise visual token compression method that integrates pixel-shuffle and residual connections, significantly improving the training and inference efficiency of MLLMs with only a minor performance drop.
- We conduct extensive experiments with different compression methods, where LaCo demonstrates superior performance and clearly stands out.
- We perform in-depth analyses by inserting LaCo at various depths of the encoder and applying different vision encoders. This exploration not only further validates the effec-

tiveness of our method but also identifies the optimal layer for internal token compression.

2 Related Works

2.1 Multimodal Large Language Models (MLLMs)

Recent advancements in MLLMs have primarily focused on the integration of LLMs with advanced visual encoders. This integration is typically achieved through a lightweight projector, facilitating the alignment of vision and language features. For instance, models such as BLIP([Li et al., 2023b](#); [Dai et al., 2023](#)), MiniGPT4([Zhu et al., 2023](#)), and QwenVL([Bai et al., 2023](#)) utilize the Q-Former (a cross-attention mechanism) to align and distill informative visual features. Flamingo([Alayrac et al., 2022](#)) introduces gated cross-attention layers to inject encoded visual information into the language model, thereby enhancing multimodal reasoning capabilities. The LLaVA series([Li et al., 2024a](#); [Liu et al., 2023a, 2024, 2023b](#)) adopts a two-layer MLP structure to bridge vision and language models, a design that has influenced subsequent models involving VILA([Lin et al., 2023](#)), ShareGPT4V([Chen et al., 2023](#)), and CogVLM([Wang et al., 2023](#)). These developments highlight the rapid evolution of MLLMs, significantly advancing their capability to handle complex multimodal tasks([Lan et al., 2025](#)).

2.2 Visual Token Compression

Visual token compression techniques have been proposed to reduce the inference complexity for MLLMs. Mainstream models, such as Qwen([Wang et al., 2024b](#)), InternVL([Chen et al., 2024d](#)), and Gemma3([Kamath et al., 2025](#)), utilize two-layer MLP models, pixel-shuffle operations, and 2D average pooling operations, respectively, to achieve visual token compression. In addition to these general approaches, several specialized methods have been designed to enhance the effectiveness of visual token compression([Lan et al., 2024](#)). TokenPacker([Li et al., 2024c](#)) downsamples visual tokens to generate queries and then employs point-to-region attention to extract information from the original tokens, thereby preserving fine-grained details in the compressed tokens. LDP([Chu et al., 2023, 2024](#)) and Abstractor([Cha et al., 2023](#)) use multi-layer convolutional structures to facilitate local token interactions while maintaining spatial relationships. Despite their advantages, these meth-

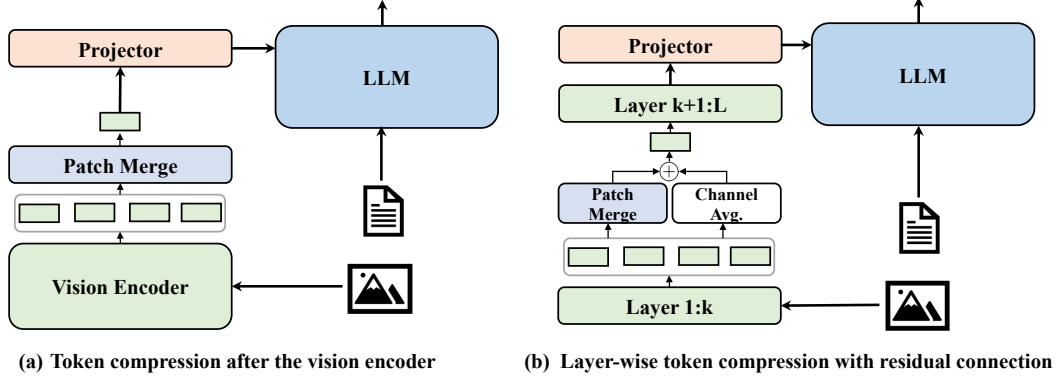


Figure 2: Comparison between encoder-level and layer-level visual token compression. The left presents compressing tokens subsequent to the encoder, which has low efficiency, while the right demonstrates compressing tokens in the intermediate layers with PML and residual connection.

ods perform compression outside the vision encoder. In contrast, our approach introduces compression within the encoder itself, enabling more efficient feature learning. Moreover, we incorporate a residual connection mechanism to mitigate information loss during compression, thereby achieving better performance with reduced computational overhead.

3 Method

In this section, we first briefly introduce how MLLMs work. Then we formulate the visual token compression problem. Afterwards, the patch merge layer with residual skip connection is proposed to mitigate the information loss problem during compression.

3.1 Multimodal Large Language Models (MLLMs)

MLLMs, typically exemplified by LLaVA(Li et al., 2024a) encompass a visual encoder, a projector, and an LLM. MLLMs process a pair of visual and textual inputs, denoted as (T, V) , where T is the textual input and V is the visual input. The visual encoder extracts features from V and converts them into N visual tokens $E_v = \{v_1, v_2, \dots, v_N\}$. These tokens are subsequently projected into the textual embedding space. The textual inputs T are mapped to M text tokens $E_t = \{t_1, t_2, \dots, t_M\}$ via the text encoder, generally $N \gg M$. The visual and text embedding are concatenated and used as input to the LLM, which performs autoregressive generation to produce the output sequence.

3.2 Visual Token Compression

Since the visual tokens have a high level of redundancy(Shang et al., 2024; Ye et al., 2024; Chen et al., 2024b), compressing visual tokens is necessary for reducing the memory usage and improving the training and inference efficiency. Formally, given a set of visual tokens E_v , a compressing module C is aimed to reduce the number of visual tokens from N to \hat{N} ($\hat{N} < N$). The compressed results are represented as $\hat{E}_v = \{\hat{v}_1, \hat{v}_2, \dots, \hat{v}_{\hat{N}}\}$:

$$C : E_v \Rightarrow \hat{E}_v, \quad (1)$$

where $N = |E_v|$, $\hat{N} = |\hat{E}_v|$ are the set size of E_v and \hat{E}_v , respectively. C is typically referred to as the patch merge layer (PML), which will be discussed in Sec3.3.

Layer-wise Token Compression. In previous methods, PML is typically placed downstream of the vision encoder, indicating that visual token compression is executed subsequent to the processing of the vision encoder. As illustrated in Fig.2, we further insert the PML within an intermediate k -th layer of the vision encoder. Specifically, assuming that the vision encoder consists of L layers, from the first to the k -th layer, the token set E_v is encoded. Immediately after the k -th layer, the PML converts E_v to \hat{E}_v , with the compression ratio r . The compressed tokens \hat{E}_v are then fed into the remaining layers from $k+1$ to L for further encoding. The process is formulated as follows:

$$\begin{aligned} E_v^k &= ENC_{1:k}(V) \\ \hat{E}_v^k &= PML(E_v^k, r) \\ \hat{E}_v &= ENC_{k+1:L}(\hat{E}_v^k), \end{aligned} \quad (2)$$

where ENC and PML represent the vision en-

coder and patch merge layer, respectively. E_v^k and \hat{E}_v^k denote the original and compressed visual token sets, which satisfies $|\hat{E}_v^k| = \frac{|E_v^k|}{r^2}$.

3.3 Patch Merge Layer (PML)

Basic Patch Merge Layer. Among existing visual token compression methods, we choose to utilize pixel-shuffle to implement the basic PML. Since it shows great performance in token reduction (Lu et al., 2025). The pixel-shuffle (Shi et al., 2016) operation first merges adjacent tokens with a grid, then a two-layer MLP is adopted to map the merged tokens back to the original embedding dimensionality:

$$\hat{E}_v = MLP(PS((E_v, r)), \quad (3)$$

where PS means the pixel-shuffle operation. For instance, E_v with shape $N \times C$ is first reshaped to $H \times W \times C$ and then converted to $\frac{H}{r} \times \frac{W}{r} \times r^2C$ by pixel-shuffle, where $H \times W = N$. After reshaped back to $\frac{N}{r^2} \times r^2C$, it is fed into the MLP and converted to $\frac{N}{r^2} \times C$, achieving the compression with ratio r .

Residual Connection. Existing visual token compression methods, such as pixel-shuffle, convolutional architectures, and TokenPacker, often suffer from the information loss problem. The problem is more pronounced when PML is placed into an intermediate layer of the vision encoder. To alleviate this limitation, motivated by Chen et al. (2024a), we propose incorporating a residual connection into the PML. Specifically, the residual pathway consists of a non-parametric shortcut realized through a space-to-channel operation, followed by a channel averaging step to align the channel dimension. The process is formulated as:

$$\hat{E}_v = RC(E_v^k, r) = CA(PS(E_v, r)), \quad (4)$$

where RC represents the residual connection and CA denotes the channel averaging operation. The process is similar to the PML but introduces no parameter. To this end, the midline in Eq. 2 is updated with:

$$\hat{E}_v^k = PML(E_v^k, r) + RC(E_v^k, r). \quad (5)$$

The PML with residual connection achieves efficient compression while mitigating the information loss.

3.4 Training Strategy

We follow the training strategies proposed in LLaVA-OneVision (Li et al., 2024a), which com-

prises three stages and is based on the curriculum learning principle of increasing difficulty gradually.

- Stage 1: *Language-Image Alignment* focuses on aligning visual features with the textual embedding space of the language model, enabling cross-modal understanding.
- Stage 1.5: *High-Quality Knowledge Learning* aims to refine the model’s generation capabilities by leveraging high-quality, curated multimodal data.
- Stage 2: *Visual Instruction Tuning* is oriented toward teaching MLLM to solve a diverse set of visual tasks with preferred responses. This stage is composed of two phases: (a) *Single-Image (SI) Training*: learning visual tasks using a single image. (b) *OneVision Training*: equipping MLLM with the abilities to process diverse inputs, such as video, single-image, and multi-image.

The first stage only learn the projector while the other two stages train MLLM with all parameters. Unlike this, due to the introduction of the inner PML, we also train the PML parameters alongside the projector during Stage 1. The remaining stages remain unchanged in our training pipeline. The training stages are depicted in Fig.3

4 Experiments

In this section, we first introduce the experiment settings. Then, we compare LaCo with other compression methods and evaluate inner-layer and external compression with various encoders. Finally, we exploit the results when placing LaCo at the different layers.

4.1 Experiment Settings

Experiments Configuration. We use three vision encoders: AIMv2 (Fini et al., 2024), SigLIP (Zhai et al., 2023), and InternViT (Chen et al., 2024e), which are widely adopted in MLLMs. The projector architecture follows the design employed in LLaVA-OneVision. We utilize Qwen2.5-0.5B as the LLM with consideration of the compute budget. All models are trained for 1 epoch with a batch size of 512. In Stage-1, the learning rate is set to be 1e-3. In both Stage 1.5 and Stage 2, the vision encoder is fine-tuned with a learning rate of 2e-6, while the remaining modules are optimized using a

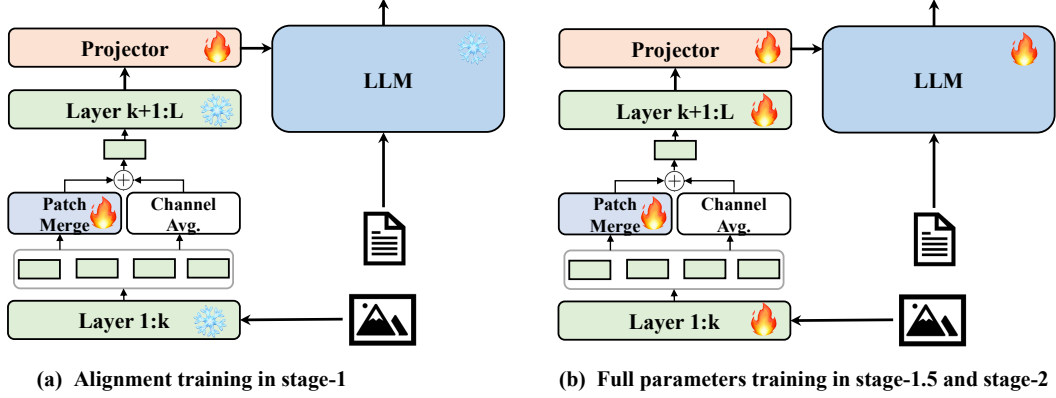


Figure 3: Detailed overview of the training stage. The left figure represents stage-1, which only learn the projector and PML. The right part depicts the stage-1.5 and stage-2, training with all parameters.

Method	PT	IT	VT	TPS	AI2D	ChartQA	DocVQA	InfoVQA	MMBench	MMMU	MMStar	S-Bench	S-QA	RW-QA	Avg.
<i>Single-Image Training Setting</i>															
Pixel-Shuffle	10.8	18.4	29.0	27.4	56.5	13.7	13.1/13.0	19.4/20.0	36.9	32.7	30.6	50.9	66.5	43.5	36.4
LDPv2	10.9	18.6	30.1	27.4	56.3	13.9	12.4/13.0	19.3/20.0	35.2	33.4	30.3	49.3	64.7	45.0	36.0
TokenPacker	11.5	20.0	33.6	26.8	56.3	13.6	12.6/13.0	19.2/20.0	35.0	32.0	30.7	49.9	66.5	44.7	36.1
LaCo	10.8	18.6	29.3	27.4	59.3	55.9	63.8/65.0	33.6/34.0	55.2	35.7	37.7	64.7	69.2	55.2	53.1
<i>One-Vision Training Setting</i>															
Pixel-Shuffle	10.8	14.1	29.4	27.5	57.6	14.0	12.0/12.0	20.4/20.0	38.8	34.1	30.7	52.2	59.3	44.4	36.3
LDPv2	10.9	13.7	29.7	27.6	57.9	14.4	12.0/12.0	20.5/20.0	36.7	33.6	28.6	51.0	62.5	45.5	36.2
TokenPacker	11.5	14.7	33.6	26.9	58.5	14.5	12.2/12.0	20.0/20.0	38.1	33.7	29.6	51.9	60.6	46.5	36.6
LaCo	10.8	13.9	29.5	27.6	61.8	59.2	62.4/64.0	34.7/34.0	58.7	35.2	39.5	62.0	66.7	55.4	53.6

Table 1: Performance comparison between Pixel-Shuffle(Chen et al., 2024d), LDPv2(Chu et al., 2024), TokenPacker(Li et al., 2024c) and LaCo on single-image benchmarks. All methods use AIMv2 as the vision encoder and place token compression methods at the 1/4 layer.

learning rate of $1e-5$. We adopt the cosine learning rate schedule with the minimum value of $1e-7$.

Baselines and Models. For baseline comparisons, we implement LaCo and three representative approaches, including Pixel-Shuffle(Chen et al., 2024d), TokenPacker(Li et al., 2024c) and the LDPv2(Chu et al., 2024). All methods are employed at the 1/4 layer of the AIMv2. We also compare inner-layer and external compression across three widely used vision encoders involving AIMv2(Fini et al., 2024), SigLIP(Zhai et al., 2023), and InternViT(Chen et al., 2024e), with LaCo applied for token compression. Furthermore, to explore the effects of compression at different layers, we place LaCo at the 1/12, 1/6, 1/4, and 1/2 layers of the vision encoder, exemplified by the AIMv2.

Training Datasets. We follow the training datasets as LLaVA-OneVision(Li et al., 2024a). In the pretrained stage-1, the LCS-558K(Liu et al., 2023b) is used to tune the projector and the PML. In the stage-1.5, we utilize the 4M high-quality knowledge data, including re-captioned detailed

description data, document/OCR data, and Chinese language data. The visual instruction tuning data for stage-2 also comes from LLaVA-OneVision, comprising 3.2M single-image instruction data in SI phase and 1.6M mixed data in one-vision phase. For some data not published, we adopt similar data under the training guidance of LLaVA-OneVision.

Evaluation Benchmarks. We evaluate our model on three different benchmark groups:

- **Single-Image Benchmarks:** including (a) *Chart, Diagram, and Document Understanding:* AI2D(Kembhavi et al., 2016), ChartQA(Masry et al., 2022), DocVQA(Mathew et al., 2020), and InfoVQA(Mathew et al., 2021); (b) *Perception and Multi-discipline Reasoning:* MMBench(Liu et al., 2023d), MMMU(Yue et al., 2024), MMStar(Chen et al., 2024c), SeedBench(image)(Li et al., 2023a), and ScienceQA(S-QA)(Saikh et al., 2022); (c) *Real-world Understanding and Visual Chat:* RealWorldQA(RW-QA)(xAI, 2024). It

Method	IEI	MI-VQA	NL-VR2	Puzzle	Q-Bench	Spot-Diff	TR-VQA	VST	3D-Chat	3D-TD	ScanQA	ALFRED	nuScenes	BLINK	Mantis	MathVerse	MuirBench	SciVerse	Avg.
	in-domain multi-image								in-domain multi-view					out-domain					
Pixel-Shuffle	27.8	72.3	63.7	35.2	47.4	38.9	58.0	29.3	60.5	48.7	26.1	60.2	57.5	38.8	38.6	26.0	27.4	26.7	43.5
LDPv2	27.3	76.2	61.9	46.1	49.0	37.2	60.1	28.6	60.5	48.5	25.2	60.3	64.2	38.2	36.1	24.4	26.2	22.0	44.0
TokenPacker	27.6	73.3	61.7	44.0	47.8	36.8	56.9	28.7	60.4	48.5	26.9	59.7	58.2	38.3	34.3	25.5	26.4	25.1	43.3
LaCo	30.0	85.0	73.2	43.9	48.5	38.8	60.5	30.6	60.5	48.9	30.3	59.7	72.5	41.3	44.4	34.3	31.9	30.4	48.0

Table 2: Performance comparison between Pixel-Shuffle(Chen et al., 2024d), the LDPv2(Chu et al., 2024), TokenPacker(Li et al., 2024c) and LaCo on multi-image benchmarks.

consists of 10 benchmarks.

- **Multi-Image Benchmarks:** including (a) *in-domain multi-image*: Spot the Difference(Jhamtani and Berg-Kirkpatrick, 2018), Image Edit Instruction(IEI)(Li et al., 2024b), Visual Storytelling(VST)(Ting-Hao et al., 2016), Text-rich VQA(TR-VQA)(Liu et al., 2023c), Multi-image VQA(MI-VQA)(Raj et al., 2021), Raven Puzzle(Chia et al., 2024), Q-Bench(Wu et al., 2023), and NLVR2(Suhr and Artzi, 2019); (b) *in-domain multi-view*: 3D Dialogue (3D-Chat) and Task Decomposition (3D-TD) from 3D-LLM(Hong et al., 2023), ScanQA(Azuma et al., 2021), ALFRED(Shridhar et al., 2019), and nuScenes(Caesar et al., 2019); (c) *out-domain tasks*: BLINK(Fu et al., 2024b), MMMU(multi-image)(Yue et al., 2024), MuirBench(Wang et al., 2024a), and MathVerse(Zhang et al., 2024). It comprises 18 benchmarks.
- **Video Benchmarks:** containing 5 benchmarks, EgoSchema(Mangalam et al., 2023), NeXTQA(Xiao et al., 2021), PerceptionTest(Puatruauecan et al., 2023), SeedBench(video)(Li et al., 2023a), and VideoMME(Fu et al., 2024a).

4.2 Main Results

Method	EgoSchema	NextQA	PercepTest	S-bench	VideoMME	Avg.
	test	mc	val	video	wo/w-sub	
Pixel-Shuffle	21.4	44.8	42.7	33.0	36.1/42.4	36.2
LDPv2	21.6	42.6	41.6	31.2	34.9/41.3	35.0
TokenPacker	22.4	45.2	41.2	31.6	36.1/41.8	35.9
LaCo	29.6	57.8	47.4	44.5	41.0/46.0	44.6

Table 3: Performance comparison between Pixel-Shuffle(Chen et al., 2024d), the LDPv2(Chu et al., 2024), TokenPacker(Li et al., 2024c) and LaCo on video benchmarks.

To validate the effectiveness of our proposed LaCo, we compare it with three representative visual token compression approaches, including

Pixel-Shuffle(Chen et al., 2024d), LDPv2(Chu et al., 2024), and TokenPacker(Li et al., 2024c). To ensure a fair comparison, all methods are applied at the 1/4 layer of the AIMv2 vision encoder, with Qwen2.5-0.5B used as the language model. All models are trained with the same data and experimental configuration.

Evaluation on Single-Image Benchmarks. As demonstrated in Tab.1, LaCo consistently outperforms the comparison methods across all evaluated scenarios. Specifically, compared to LaCo, Pixel-Shuffle, LDPv2, and TokenPacker exhibit performance dropping by over 30% in terms of average metrics in both single-training and one-vision training. Although they demonstrate competitive performance when applied externally, their effectiveness diminishes significantly when used to compress tokens in the intermediate layers of vision encoders, highlighting the superiority of our layer-wise design. LaCo further improves upon Pixel-Shuffle by introducing residual connections, which play a critical role in preserving informative visual features during compression. Notably, on challenging benchmarks such as DocVQA(Mathew et al., 2020), InfoVQA(Mathew et al., 2021), and MMBench(Liu et al., 2023d), where accurate task completion heavily relies on rich contextual information, Pixel-Shuffle, LDPv2, and TokenPacker suffer from significant performance degradation due to substantial information loss. This further indicates the effectiveness of LaCo in preserving critical visual content during token compression. Moreover, we present extensive case studies in the Appendix.A to demonstrate the superiority of LaCo in handling diverse complex tasks.

We also report the efficiency of these methods in terms of **Pre-training Time (PT)**, **Instruction Tuning Time (IT)**, **Vision Encode Time (VT)**, and **Tokens Per Second (TPS)**, where PT and IT evaluate training efficiency, VT and TPS quantify inference efficiency. TokenPacker exhibits the lowest overall efficiency, while LDPv2, Pixel-shuffle,

Model	PT	IT	VT	TPS	A12D	ChartQA	DocVQA	InfoVQA	MMBench	MMMU	MMStar	S-Bench	S-QA	RW-QA	Avg
<i>Single-Image Training Setting</i>															
SigLIP-LaCo@1	14.5	29.6	146.5	18.0	56.5	13.0	12.2/12.0	19.9/20.0	27.1	32.8	27.2	44.0	62.5	46.7	34.2
SigLIP-LaCo@1/4	11.9	22.2	57.3	24.0	56.8	13.3	12.3/13.0	19.6/20.0	40.1	33.1	33.2	55.4	65.1	45.2	37.5
InViT-LaCo@1	14.0	28.6	107.6	19.0	60.8	67.5	76.6/76.0	41.7/41.1	56.1	36.2	38.6	65.2	70.3	54.2	56.7
InViT-LaCo@1/4	12.3	22.3	43.4	25.5	59.2	59.7	68.8/70.0	34.6/35.0	52.9	34.8	38.9	62.6	69.2	51.1	53.3
AIMv2-LaCo@1	11.7	25.8	58.0	24.0	60.9	63.2	73.5/74.0	39.6/39.0	55.6	35.1	38.6	66.4	70.7	56.1	56.0
AIMv2-LaCo@1/4	10.8	19.3	29.3	27.4	59.3	55.9	63.8/65.0	33.6/34.0	55.2	35.7	37.7	64.7	69.2	55.2	53.1
<i>One-Vision Training Setting</i>															
SigLIP-LaCo@1	14.5	26.5	146.3	18.2	57.4	13.8	11.8/12.0	20.1/20.0	34.6	34.4	30.8	47.1	52.5	45.0	34.8
SigLIP-LaCo@1/4	11.9	15.8	57.4	24.8	57.9	15.9	11.7/12.0	20.1/20.0	47.9	34.4	33.8	57.8	60.4	46.0	38.6
InViT-LaCo@1	14.0	23.2	107.7	19.0	62.5	69.5	75.3/76.0	41.2/41.0	57.9	34.9	40.7	66.9	65.5	54.5	56.9
InViT-LaCo@1/4	12.3	16.2	43.7	24.8	61.0	61.7	66.9/68.0	36.1/36.0	54.9	36.2	38.9	65.3	67.6	52.2	54.1
AIMv2-LaCo@1	11.7	18.9	57.6	24.0	62.2	65.6	71.8/73.0	40.1/41.0	60.1	36.2	40.9	67.9	64.3	54.2	56.4
AIMv2-LaCo@1/4	10.8	13.9	29.5	27.6	61.8	59.2	62.4/64.0	34.7/34.0	58.7	35.2	39.5	62.0	66.7	55.4	53.6

Table 4: Performance comparison between LaCo@1/4 and LaCo@1 in AIMv2(Fini et al., 2024), SigLIP(Zhai et al., 2023), and InternViT(Chen et al., 2024e) on single-image benchmarks. LaCo@x means placing LaCo at the x-th layer of the vision encoder.

and LaCo demonstrate comparable performance in terms of efficiency. However, our LaCo achieves significantly better results in effectiveness while maintaining high efficiency.

Evaluation on Multi-Image Benchmarks. For multi-image benchmarks, the models evaluated are identical to those used in the single-image setting. Therefore, we omit the efficiency metrics in Tab. 2 for brevity. As seen from the table, LaCo achieves superior performance compared to methods Pixel-Shuffle, LDPv2, and TokenPacker, surpassing them by 10.3%, 9.1%, and 10.9% respectively in average benchmark metrics. This fully demonstrates the effectiveness of LaCo in handling complex tasks such as multi-image reasoning, identifying differences, and understanding 3D environments.

Evaluation on Video Benchmarks. Tab.3 demonstrates the results on video benchmarks. LaCo outperforms Pixel-Shuffle, LDPv2, and TokenPacker by 23.2%, 27.4%, and 24.2%, respectively, in comparative evaluations. The results highlight the superiority of LaCo in handling temporal-spatial information.

4.3 LaCo for Different Encoders

To evaluate the generalization capability and efficiency improvements of our approach, we further conduct experiments using three vision encoders involving AIMv2, SigLIP, and InternViT (referred to as InViT). We compare token compression performed within an intermediate layer of the vision encoder to compression applied externally. Specifically, we apply our proposed LaCo both at the 1/4

layer of the encoder and subsequent to the encoder. Qwen2.5-0.5B is used as the LLM. All experiments are conducted with the same training data and configuration to ensure a fair comparison.

As shown in Tab. 4, AIMv2-LaCo@1/4 achieves 7.7% improvement in PT, 26.5% in IT, 48.8% in VT, and 15.0% in TPS compared to compared to AIMv2-LaCo@1 (LaCo applied subsequent to the encoder). Similarly, when applied to SigLIP and InternViT, the training and inference efficiency improvements reach 29.3%-26.6% and 22.8%-30.5%, respectively. In terms of effectiveness, the results show mixed outcomes. For SigLIP, inner-layer compression (LaCo@1/4) outperforms external compression by 2.7 in average accuracy. AIMv2 and InternViT both exhibit slight declines, decreasing by 5.0% and 4.9%, respectively. Specifically, performance drops much only on DocVQA, InfoVQA, and ChartQA benchmarks while even gets improved on ScienceQA and RealWordQA. We attribute this phenomenon to the fact that tasks on DocVQA, InfoVQA, and ChartQA require rich and fine-grained visual information to achieve good results. Inner-layer compression inevitably reduces more information than external compression, thus performing worse. However, it is still useful to apply inner-layer token compression when the compute budget is limited.

For multi-image benchmarks, Tab. 5 shows the detailed results. As seen from the table, the performance gap between inner-layer and external compression narrows significantly under the multi-image setup, which can be verified on both AIMv2,

Model	IEI	ML-VQA	NL-VR2	Puzzle	Q-Bench	Spot-Diff	TR-VQA	VST	3D-Chat	3D-TD	ScanQA	ALFRED	nuScenes	BLINK	Mantis	MathVerse	MuirBench	SidVerse	Avg.
	in-domain multi-image								in-domain multi-view					out-domain					
SigLIP-LaCo@1	26.9	67.5	58.1	35.4	48.2	34.8	57.0	29.2	60.5	48.4	19.8	58.0	55.8	38.7	42.2	25.0	24.9	25.6	42.0
SigLIP-LaCo@1/4	28.4	78.0	67.4	28.9	48.3	37.3	58.2	29.6	60.5	48.7	25.5	59.6	62.2	38.5	39.0	30.8	31.3	26.0	44.3
InViT-LaCo@1	29.4	81.0	73.8	37.6	49.5	40.1	64.6	30.3	60.8	49.1	30.1	57.5	72.8	40.5	43.5	36.3	34.8	40.0	48.4
InViT-LaCo@1/4	29.3	80.2	72.3	36.9	47.3	37.9	61.6	30.2	60.8	48.8	30.0	56.3	75.3	39.6	43.5	44.8	33.2	49.6	48.8
AIMv2-LaCo@1	30.4	82.8	75.7	42.4	49.9	37.3	66.1	30.2	60.6	49.1	31.3	59.5	73.0	40.5	44.9	42.5	35.9	41.8	49.7
AIMv2-LaCo@1/4	30.0	85.0	73.2	43.9	48.5	38.8	60.5	30.6	60.5	48.9	30.3	59.7	72.5	41.3	44.4	34.3	31.9	30.4	48.0

Table 5: Performance comparison between LaCo@1/4 and LaCo@1 in AIMv2(Fini et al., 2024), SigLIP(Zhai et al., 2023), and InternViT(Chen et al., 2024e) on multi-image benchmarks.

Model	EgoSchema	NextQA	PercepTest	S-bench	VideoMME	Avg.
	test	mc	val	video	wo/w-sub	
SigLIP-LaCo@1	20.6	40.4	41.6	31.4	36.1/41.0	34.5
SigLIP-LaCo@1/4	23.3	49.6	43.2	34.6	37.3/44.3	37.9
InViT-LaCo@1	29.0	61.4	46.8	45.8	43.6/47.8	45.7
InViT-LaCo@1/4	27.8	59.9	46.9	40.6	42.2/46.6	43.9
AIMv2-LaCo@1	30.0	61.6	47.9	47.4	43.1/ 48.1	46.5
AIMv2-LaCo@1/4	29.6	57.8	47.4	44.5	41.0/46.0	44.6

Table 6: Performance comparison between LaCo@1/4 and LaCo@1 in AIMv2(Fini et al., 2024), SigLIP(Zhai et al., 2023), and InternViT(Chen et al., 2024e) on video benchmarks.

SigLIP, and InternViT encoders. Among the three encoders, AIMv2 gets the best performance while SigLIP ranks relatively lower.

Tab.6 demonstrates the results on video benchmarks. While inner-layer compression still has room for improvement compared to external token compression, it delivers competitive performance while significantly improving training efficiency. This suggests that our method has strong potential for deployment in resource-constrained scenarios involving long visual sequences such as videos.

4.4 LaCo at Different Layers

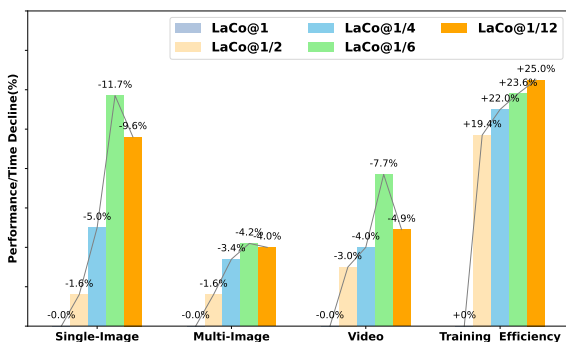


Figure 4: The percentages of performance and training time decline when compressing tokens in the inner layers of AIMv2. AIMv2-LaCo@x means placing LaCo at the x-th layer of AIMv2.

To further investigate the trade-off between per-

formance and efficiency when placing LaCo at different depths of the vision encoder, we conduct experiments using AIMv2 as the vision encoder and Qwen2.5-0.5B as the language model. Specifically, LaCo is inserted at four distinct layers—1/12, 1/6, 1/4, and 1/2 of the total encoder depth for visual token compression. For a fair comparison, all models are trained under identical data and experimental settings.

As shown in Fig.4, we summarize the relative performance drop across different compression layers, represented by the first three bar groups. The last group illustrates the corresponding increase in training efficiency. From the results, we observe that compressing visual tokens within intermediate layers improves training efficiency by over 20%, despite some performance degradation. Moreover, as the compression layer decreases, performance drops more rapidly, whereas training efficiency gains become increasingly marginal. It’s a good idea to choose to compress tokens in the 1/2 layer of the vision encoder, striking a balance between performance and efficiency. It is worth noting that compressing tokens at the 1/12 layer achieves higher performance compared to compression at the 1/6 layer. This indicates that early compression preserves more useful visual information when compressing at shallower layers ($\leq 1/6$) of the vision encoder. In addition, we give the detailed evaluation results of layer-wise and external token compression in Appendix.B.

Conclusions

We demonstrate that compressing visual tokens within the intermediate layers of the vision encoder holds significant potential for improving the efficiency of MLLMs. To this end, we propose LaCo, a novel token compression method that leverages pixel-shuffle operations and residual connections to merge visual tokens with minimal information

loss. Experimental results clearly validate the effectiveness of our approach, showing over a 20% improvement in training efficiency while maintaining strong performance—surpassing existing methods in terms of information preservation. Nonetheless, several directions remain open for future exploration. For instance, investigating adaptive compression ratios r across different layers or tasks could further enhance flexibility and performance. Additionally, scaling the language model to larger architectures may unlock new capabilities when combined with our compression strategy. We plan to explore these avenues in our future work.

Limitations

The primary limitation of LaCo is its relatively weaker performance when applied in inner-layer compression than when applied externally. However, it is beneficial for its lower training and inference cost while maintaining the strong performance of MLLMs. Therefore, a method for further enhancing the performance of layer-wise token compression should be explored.

References

- Jean-Baptiste Alayrac, Jeff Donahue, Pauline Luc, Antoine Miech, Iain Barr, Yana Hasson, Karel Lenc, Arthur Mensch, Katie Millican, Malcolm Reynolds, Roman Ring, Eliza Rutherford, Serkan Cabi, Tengda Han, Zhitao Gong, Sina Samangooei, Marianne Monteiro, Jacob Menick, Sebastian Borgeaud, and 8 others. 2022. Flamingo: a visual language model for few-shot learning. *ArXiv*, abs/2204.14198.
- Daichi Azuma, Taiki Miyanishi, Shuhei Kurita, and Motoaki Kawanabe. 2021. Scanqa: 3d question answering for spatial scene understanding. *2022 IEEE/CVF Conference on Computer Vision and Pattern Recognition (CVPR)*, pages 19107–19117.
- Jinze Bai, Shuai Bai, Shusheng Yang, Shijie Wang, Sinan Tan, Peng Wang, Junyang Lin, Chang Zhou, and Jingren Zhou. 2023. Qwen-vl: A frontier large vision-language model with versatile abilities. *ArXiv*, abs/2308.12966.
- Holger Caesar, Varun Bankiti, Alex H. Lang, Sourabh Vora, Venice Erin Liong, Qiang Xu, Anush Krishnan, Yuxin Pan, Giancarlo Baldan, and Oscar Beijbom. 2019. nuscenes: A multimodal dataset for autonomous driving. *2020 IEEE/CVF Conference on Computer Vision and Pattern Recognition (CVPR)*, pages 11618–11628.
- Junbum Cha, Wooyoung Kang, Jonghwan Mun, and Byungseok Roh. 2023. Honeybee: Locality-enhanced projector for multimodal llm. *2024 IEEE/CVF Conference on Computer Vision and Pattern Recognition (CVPR)*, pages 13817–13827.
- Junyu Chen, Han Cai, Junsong Chen, Enze Xie, Shang Yang, Haotian Tang, Muyang Li, Yao Lu, and Song Han. 2024a. Deep compression autoencoder for efficient high-resolution diffusion models. *ArXiv*, abs/2410.10733.
- Liang Chen, Haozhe Zhao, Tianyu Liu, Shuai Bai, Junyang Lin, Chang Zhou, and Baobao Chang. 2024b. An image is worth 1/2 tokens after layer 2: Plug-and-play inference acceleration for large vision-language models. In *European Conference on Computer Vision*.
- Lin Chen, Jinsong Li, Xiao wen Dong, Pan Zhang, Conghui He, Jiaqi Wang, Feng Zhao, and Dahua Lin. 2023. Sharegpt4v: Improving large multi-modal models with better captions. In *European Conference on Computer Vision*.
- Lin Chen, Jinsong Li, Xiao wen Dong, Pan Zhang, Yuhang Zang, Zehui Chen, Haodong Duan, Jiaqi Wang, Yu Qiao, Dahua Lin, and Feng Zhao. 2024c. Are we on the right way for evaluating large vision-language models? *ArXiv*, abs/2403.20330.
- Zhe Chen, Weiyun Wang, Hao Tian, Shenglong Ye, Zhangwei Gao, Erfei Cui, Wenwen Tong, Kongzhi Hu, Jiapeng Luo, Zheng Ma, Ji Ma, Jiaqi Wang, Xiao wen Dong, Hang Yan, Hewei Guo, Conghui He, Zhenjiang Jin, Chaochao Xu, Bin Wang, and 9 others. 2024d. How far are we to gpt-4v? closing the gap to commercial multimodal models with open-source suites. *ArXiv*, abs/2404.16821.
- Zhe Chen, Jiannan Wu, Wenhai Wang, Weijie Su, Guo Chen, Sen Xing, Muyan Zhong, Qinglong Zhang, Xizhou Zhu, Lewei Lu, Bin Li, Ping Luo, Tong Lu, Yu Qiao, and Jifeng Dai. 2024e. Internvl: Scaling up vision foundation models and aligning for generic visual-linguistic tasks. *Preprint*, arXiv:2312.14238.
- Yew Ken Chia, Vernon Toh Yan Han, Deepanway Ghosal, Lidong Bing, and Soujanya Poria. 2024. Puzzlevqa: Diagnosing multimodal reasoning challenges of language models with abstract visual patterns. *ArXiv*, abs/2403.13315.
- Xiangxiang Chu, Limeng Qiao, Xinyang Lin, Shuang Xu, Yang Yang, Yiming Hu, Fei Wei, Xinyu Zhang, Bo Zhang, Xiaolin Wei, and Chunhua Shen. 2023. Mobilevlm : A fast, strong and open vision language assistant for mobile devices. *ArXiv*, abs/2312.16886.
- Xiangxiang Chu, Limeng Qiao, Xinyu Zhang, Shuang Xu, Fei Wei, Yang Yang, Xiaofei Sun, Yiming Hu, Xinyang Lin, Bo Zhang, and Chunhua Shen. 2024. Mobilevlm v2: Faster and stronger baseline for vision language model. *ArXiv*, abs/2402.03766.
- Wenliang Dai, Junnan Li, Dongxu Li, Anthony Meng Huat Tiong, Junqi Zhao, Weisheng Wang, Boyang Albert Li, Pascale Fung, and Steven C. H. Hoi. 2023. Instructblip: Towards general-purpose vision-language models with instruction tuning. *ArXiv*, abs/2305.06500.

- Enrico Fini, Mustafa Shukor, Xiujun Li, Philipp Dufter, Michal Klein, David Haldimann, Sai Aitharaju, Victor Guilherme Turrisi da Costa, Louis B'ethune, Zhe Gan, Alexander Toshev, Marcin Eichner, Moin Nabi, Yinfei Yang, Joshua M. Susskind, and Alaaeldin El-Nouby. 2024. Multimodal autoregressive pre-training of large vision encoders. *ArXiv*, abs/2411.14402.
- Chaoyou Fu, Yuhan Dai, Yondong Luo, Lei Li, Shuhuai Ren, Renrui Zhang, Zihan Wang, Chenyu Zhou, Yunhang Shen, Mengdan Zhang, Peixian Chen, Yanwei Li, Shaohui Lin, Sirui Zhao, Ke Li, Tong Xu, Xiwu Zheng, Enhong Chen, Rongrong Ji, and Xing Sun. 2024a. Video-mme: The first-ever comprehensive evaluation benchmark of multi-modal llms in video analysis. *ArXiv*, abs/2405.21075.
- Xingyu Fu, Yushi Hu, Bangzheng Li, Yu Feng, Haoyu Wang, Xudong Lin, Dan Roth, Noah A. Smith, Wei-Chiu Ma, and Ranjay Krishna. 2024b. Blink: Multimodal large language models can see but not perceive. *ArXiv*, abs/2404.12390.
- Yining Hong, Haoyu Zhen, Peihao Chen, Shuhong Zheng, Yilun Du, Zhenfang Chen, and Chuang Gan. 2023. 3d-llm: Injecting the 3d world into large language models. *ArXiv*, abs/2307.12981.
- Harsh Jhamtani and Taylor Berg-Kirkpatrick. 2018. Learning to describe differences between pairs of similar images. *ArXiv*, abs/1808.10584.
- Gemma Team Aishwarya Kamath, Johan Ferret, Shreya Pathak, Nino Vieillard, Ramona Merhej, Sarah Perrin, Tatiana Matejovicova, Alexandre Ram'e, Morgane Rivière, Louis Rouillard, Thomas Mesnard, Geoffrey Cideron, Jean-Bastien Grill, Sabela Ramos, Edouard Yvinec, Michelle Casbon, Etienne Pot, Ivo Penchev, Gael Liu, and 191 others. 2025. Gemma 3 technical report. *ArXiv*, abs/2503.19786.
- Aniruddha Kembhavi, Michael Salvato, Eric Kolve, Minjoon Seo, Hannaneh Hajishirzi, and Ali Farhadi. 2016. A diagram is worth a dozen images. *ArXiv*, abs/1603.07396.
- Zhibin Lan, Liqiang Niu, Fandong Meng, Wenbo Li, Jie Zhou, and Jinsong Su. 2024. Avg-llava: A large multimodal model with adaptive visual granularity. *ArXiv*, abs/2410.02745.
- Zhibin Lan, Liqiang Niu, Fandong Meng, Jie Zhou, and Jinsong Su. 2025. Llave: Large language and vision embedding models with hardness-weighted contrastive learning. *ArXiv*, abs/2503.04812.
- Bo Li, Yuanhan Zhang, Dong Guo, Renrui Zhang, Feng Li, Hao Zhang, Kaichen Zhang, Yanwei Li, Ziwei Liu, and Chunyuan Li. 2024a. Llava-onevision: Easy visual task transfer. *ArXiv*, abs/2408.03326.
- Bohao Li, Rui Wang, Guangzhi Wang, Yuying Ge, Yixiao Ge, and Ying Shan. 2023a. Seed-bench: Benchmarking multimodal llms with generative comprehension. *ArXiv*, abs/2307.16125.
- Feng Li, Renrui Zhang, Hao Zhang, Yuanhan Zhang, Bo Li, Wei Li, Zejun Ma, and Chunyuan Li. 2024b. Llava-next-interleave: Tackling multi-image, video, and 3d in large multimodal models. *ArXiv*, abs/2407.07895.
- Junnan Li, Dongxu Li, Silvio Savarese, and Steven C. H. Hoi. 2023b. Blip-2: Bootstrapping language-image pre-training with frozen image encoders and large language models. In *International Conference on Machine Learning*.
- Wentong Li, Yuqian Yuan, Jian Liu, Dongqi Tang, Song Wang, Jianke Zhu, and Lei Zhang. 2024c. Token-packer: Efficient visual projector for multimodal llm. *ArXiv*, abs/2407.02392.
- Ji Lin, Hongxu Yin, Wei Ping, Yao Lu, Pavlo Molchanov, Andrew Tao, Huizi Mao, Jan Kautz, Mohammad Shoeybi, and Song Han. 2023. Vila: On pre-training for visual language models. *2024 IEEE/CVF Conference on Computer Vision and Pattern Recognition (CVPR)*, pages 26679–26689.
- Haotian Liu, Chunyuan Li, Yuheng Li, and Yong Jae Lee. 2023a. Improved baselines with visual instruction tuning. *2024 IEEE/CVF Conference on Computer Vision and Pattern Recognition (CVPR)*, pages 26286–26296.
- Haotian Liu, Chunyuan Li, Yuheng Li, Bo Li, Yuanhan Zhang, Sheng Shen, and Yong Jae Lee. 2024. Llava-next: Improved reasoning, ocr, and world knowledge.
- Haotian Liu, Chunyuan Li, Qingyang Wu, and Yong Jae Lee. 2023b. Visual instruction tuning. *ArXiv*, abs/2304.08485.
- Xuejing Liu, Wei Tang, Xinzhe Ni, Jinghui Lu, Rui Zhao, Zechao Li, and Fei Tan. 2023c. What large language models bring to text-rich vqa? *ArXiv*, abs/2311.07306.
- Yuanzhan Liu, Haodong Duan, Yuanhan Zhang, Bo Li, Songyang Zhang, Wangbo Zhao, Yike Yuan, Jiaqi Wang, Conghui He, Ziwei Liu, Kai Chen, and Dahua Lin. 2023d. Mmbench: Is your multi-modal model an all-around player? In *European Conference on Computer Vision*.
- Dongchen Lu, Yuyao Sun, Zilu Zhang, Leping Huang, Jianliang Zeng, Mao Shu, and Huo Cao. 2025. Internvl-x: Advancing and accelerating internvl series with efficient visual token compression. *ArXiv*, abs/2503.21307.
- Karttikeya Mangalam, Raiymbek Akshulakov, and Jitendra Malik. 2023. Egoschema: A diagnostic benchmark for very long-form video language understanding. *ArXiv*, abs/2308.09126.
- Ahmed Masry, Do Xuan Long, Jia Qing Tan, Shafiq R. Joty, and Enamul Hoque. 2022. Chartqa: A benchmark for question answering about charts with visual and logical reasoning. *ArXiv*, abs/2203.10244.

- Minesh Mathew, Viraj Bagal, Rubèn Pérez Tito, Dimosthenis Karatzas, Ernest Valveny, and C.V. Jawahar. 2021. Infographicvqa. *2022 IEEE/CVF Winter Conference on Applications of Computer Vision (WACV)*, pages 2582–2591.
- Minesh Mathew, Dimosthenis Karatzas, R. Manmatha, and C. V. Jawahar. 2020. Docvqa: A dataset for vqa on document images. *2021 IEEE Winter Conference on Applications of Computer Vision (WACV)*, pages 2199–2208.
- Viorica Patruaicean, Lucas Smaira, Ankush Gupta, Adrià Recasens Contente, Larisa Markeeva, Dylan Banarse, Skanda Koppula, Joseph Heyward, Mateusz Malinowski, Yezhou Yang, Carl Doersch, Tatiana Matejovicova, Yury Sulsky, Antoine Miech, Alexander Fréchet, Hanna Klimczak, R. Koster, Junlin Zhang, Stephanie Winkler, and 5 others. 2023. Perception test: A diagnostic benchmark for multimodal video models. *ArXiv*, abs/2305.13786.
- Harsh Raj, Janhavi Dadhanania, and Akhilesh Bhardwaj. 2021. Multi-image visual question answering. *ArXiv*, abs/2112.13706.
- Tanik Saikh, Tirthankar Ghosal, Amish Mittal, Asif Ekbal, and Pushpak Bhattacharyya. 2022. Scienceqa: a novel resource for question answering on scholarly articles. *International Journal on Digital Libraries*, 23:289 – 301.
- Yuzhang Shang, Mu Cai, Bingxin Xu, Yong Jae Lee, and Yan Yan. 2024. Llava-prumerge: Adaptive token reduction for efficient large multimodal models. *ArXiv*, abs/2403.15388.
- Wenzhe Shi, Jose Caballero, Ferenc Huszár, Johannes Totz, Andrew P. Aitken, Rob Bishop, Daniel Rueckert, and Zehan Wang. 2016. Real-time single image and video super-resolution using an efficient subpixel convolutional neural network. *2016 IEEE Conference on Computer Vision and Pattern Recognition (CVPR)*, pages 1874–1883.
- Mohit Shridhar, Jesse Thomason, Daniel Gordon, Yonatan Bisk, Winson Han, Roozbeh Mottaghi, Luke Zettlemoyer, and Dieter Fox. 2019. Alfred: A benchmark for interpreting grounded instructions for everyday tasks. *2020 IEEE/CVF Conference on Computer Vision and Pattern Recognition (CVPR)*, pages 10737–10746.
- Alane Suhr and Yoav Artzi. 2019. Nlvr2 visual bias analysis. *ArXiv*, abs/1909.10411.
- Ting-Hao, Huang, Francis Ferraro, Nasrin Mostafazadeh, Ishan Misra, Aishwarya Agrawal, Jacob Devlin, Ross Girshick, Xiaodong He, Pushmeet Kohli, Dhruv Batra, C. Lawrence Zitnick, Devi Parikh, Lucy Vanderwende, Michel Galley, and Margaret Mitchell. 2016. *Visual storytelling*. Preprint, arXiv:1604.03968.
- Fei Wang, Xingyu Fu, James Y. Huang, Zekun Li, Qin Liu, Xiaogeng Liu, Mingyu Derek Ma, Nan Xu, Wenxuan Zhou, Kai Zhang, Tianyi Yan, Wenjie Jacky Mo, Hsiang-Hui Liu, Pan Lu, Chunyuan Li, Chaowei Xiao, Kai-Wei Chang, Dan Roth, Sheng Zhang, and 2 others. 2024a. Muirbench: A comprehensive benchmark for robust multi-image understanding. *ArXiv*, abs/2406.09411.
- Peng Wang, Shuai Bai, Sinan Tan, Shijie Wang, Zhihao Fan, Jinze Bai, Ke-Yang Chen, Xuejing Liu, Jialin Wang, Wenbin Ge, Yang Fan, Kai Dang, Mengfei Du, Xuancheng Ren, Rui Men, Dayiheng Liu, Chang Zhou, Jingren Zhou, and Junyang Lin. 2024b. Qwen2-vl: Enhancing vision-language model’s perception of the world at any resolution. *ArXiv*, abs/2409.12191.
- Weihan Wang, Qingsong Lv, Wenmeng Yu, Wenyi Hong, Ji Qi, Yan Wang, Junhui Ji, Zhuoyi Yang, Lei Zhao, Xixuan Song, Jiazheng Xu, Bin Xu, Juanzi Li, Yuxiao Dong, Ming Ding, and Jie Tang. 2023. Cogvlm: Visual expert for pretrained language models. *ArXiv*, abs/2311.03079.
- Haoning Wu, Zicheng Zhang, Erli Zhang, Chaofeng Chen, Liang Liao, Annan Wang, Chunyi Li, Wenxiu Sun, Qiong Yan, Guangtao Zhai, and Weisi Lin. 2023. Q-bench: A benchmark for general-purpose foundation models on low-level vision. *ArXiv*, abs/2309.14181.
- xAI. 2024. Grok-1.5. A Large Language Model (LLM) developed by xAI.
- Junbin Xiao, Xindi Shang, Angela Yao, and Tat seng Chua. 2021. Next-qa: Next phase of question-answering to explaining temporal actions. *2021 IEEE/CVF Conference on Computer Vision and Pattern Recognition (CVPR)*, pages 9772–9781.
- Weihao Ye, Qiong Wu, Wenhao Lin, and Yiyi Zhou. 2024. Fit and prune: Fast and training-free visual token pruning for multi-modal large language models. *ArXiv*, abs/2409.10197.
- Xiang Yue, Tianyu Zheng, Yuansheng Ni, Yubo Wang, Kai Zhang, Shengbang Tong, Yuxuan Sun, Ming Yin, Botao Yu, Ge Zhang, Huan Sun, Yu Su, Wenhu Chen, and Graham Neubig. 2024. Mmmu-pro: A more robust multi-discipline multimodal understanding benchmark. *ArXiv*, abs/2409.02813.
- Xiaohua Zhai, Basil Mustafa, Alexander Kolesnikov, and Lucas Beyer. 2023. Sigmoid loss for language image pre-training. *2023 IEEE/CVF International Conference on Computer Vision (ICCV)*, pages 11941–11952.
- Renrui Zhang, Dongzhi Jiang, Yichi Zhang, Haokun Lin, Ziyu Guo, Pengshuo Qiu, Aojun Zhou, Pan Lu, Kai-Wei Chang, Peng Gao, and Hongsheng Li. 2024. Mathverse: Does your multi-modal llm truly see the diagrams in visual math problems? In *European Conference on Computer Vision*.
- Deyao Zhu, Jun Chen, Xiaoqian Shen, Xiang Li, and Mohamed Elhoseiny. 2023. Minigt-4: Enhancing

vision-language understanding with advanced large language models. *ArXiv*, abs/2304.10592.

A Visual Results

To further validate the practical effectiveness of our approach in visual comprehension, we evaluate it on diverse real-world tasks requiring complex reasoning, as demonstrated in Fig. 5. Equipped with pixel-shuffle and residual connections, LaCo demonstrates superior performance across challenging scenarios, consistently outperforming existing methods like Pixel-Shuffle, LDPv2, and TokenPacker. This aligns with findings that information-aware designs enhance practical applicability in multimodal tasks, particularly in tasks demanding rich contextual understanding.

B Detailed Evaluation of Layer-wise Compression

We detail the evaluation of the experimental results applying our proposed LaCo at the different layers of AIMv2. The results are demonstrated on Tab.8, Tab.9, and Tab.7, which represent the model performance on single-image, multi-image, and video benchmarks, respectively.

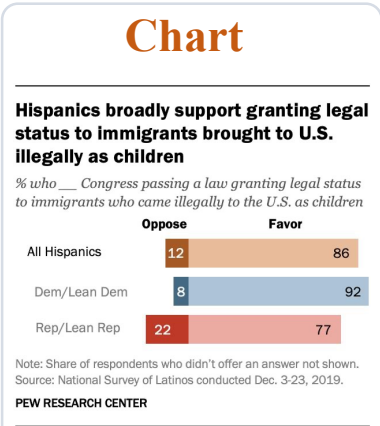
Specifically, Tab.8 shows the performance of applying LaCo at different layers of AIMv2 on single-image benchmarks. From the table, we observe that compressing tokens within the encoder leads to a training and inference efficiency improvement exceeding 20% and 10%, respectively. Furthermore, as the compression layer is placed closer to the input (i.e., at shallower layers), the acceleration effect becomes more pronounced. Compared to external token compression, when performing token compression within the encoder, the model exhibits a more significant performance drop on three benchmarks: ChartQA, DocVQA, and InfoVQA. However, its performance remains comparable or even surpasses that of external compression on other benchmarks, particularly showing improved results on benchmarks MME and RealWorldQA. This is because tasks ChartQA, DocVQA, and InfoVQA require detailed information for reasoning, and internal compression inevitably leads to some loss of information, resulting in performance degradation.

As shown in Tab.9, while layer-wise token compression still has room for improvement compared to external compression, it achieves competitive performance on most multi-image benchmarks. Internal compression exhibits a significant performance drop only on MathVerse, MuirBench, and SciVerse, which are relatively more challenging and require rich information for reasoning. Tab.7

demonstrates the performance on video benchmarks. Compared to external compression, layer-wise compression achieves comparable results.

Method	EgoSchema	NextQA	PercepTest	S-bench	VideoMME	Avg.
	test	mc	val	video	wo/w-sub	
LaCo@1/12	29.5	59.5	46.7	41.7	40.6/46.1	44.2
LaCo@1/6	26.2	57.3	46.6	42.3	39.2/45.3	42.9
LaCo@1/4	29.6	57.8	47.4	44.5	41.0/46.0	44.6
LaCo@1/2	29.1	59.8	47.6	44.3	42.7/46.7	45.1
LaCo@1	30.0	61.6	47.9	47.4	43.1/48.1	46.5

Table 7: Performance and efficiency comparison between LaCo@1/12, LaCo@1/6, LaCo@1/4, LaCo@1/2 and LaCo@1 on video benchmarks.



Q: What is the value of Favor on the blue bar?

Pixel-Shuffle: 0.46 LDPv2: 0.45

TokenPacker: 41 LaCo: 92

Count



Q: How many burgers are in this photo?
A. Two. B. Three. C. One.

Pixel-Shuffle: C LDPv2: C

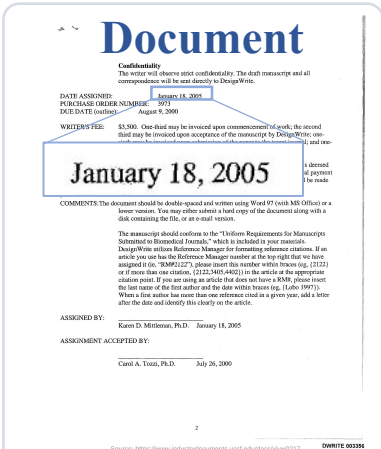
TokenPacker: C LaCo: A



Q: How many animals are in this photo?
A. Eight. B. Nine. C. One.

Pixel-Shuffle: A LDPv2: A

TokenPacker: A LaCo: B



Q: What is the Date Assigned as per the document?

Pixel-Shuffle: 10/26/98

LDPv2: 10/26/95

TokenPacker: 10/26/97

LaCo: January 18, 2005

Visual Perception



Q: Which direction is the arrow pointing?

Pixel-Shuffle: Right

LDPv2: Right

TokenPacker: Right

LaCo: Left



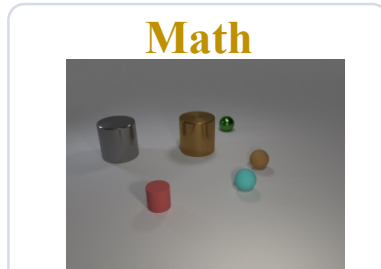
Q: Which red tree is the smallest?

Pixel-Shuffle: The middle One.

LDPv2: The front one.

TokenPacker: The front one.

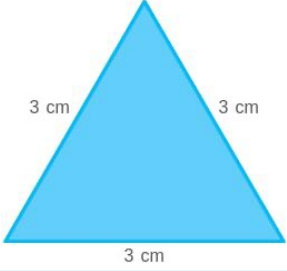
LaCo: The farthest one.



Q: Subtract all red things. Subtract all cylinders. How many objects are left?

Pixel-Shuffle: 4 LDPv2: 4

TokenPacker: 4 LaCo: 3

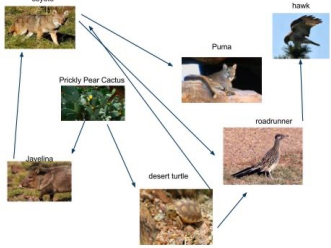


Q: What is the perimeter of the shape?

Pixel-Shuffle: 18 LDPv2: 12

TokenPacker: 12 LaCo: 9

Science



Q: According to the given food web, what is the producer?
["prickly pear cactus", "javelina", "desert turtle", "coyote"]

Pixel-Shuffle: coyote

LDPv2: desert turtle

TokenPacker: coyote

LaCo: prickly pear cactus

Figure 5: Visual comparison between Pixel-Shuffle(Chen et al., 2024d), LDPv2(Chu et al., 2024), TokenPacker(Li et al., 2024c) and LaCo. Red fonts denote the wrong answers.

Method	PT	IT	VT	TPS	A12D	ChartQA	DocVQA	InfoVQA	MMBench	MMMU	MMStar	S-Bench	S-QA	RW-QA	Avg.
<i>Single-Image Training Setting</i>															
LaCo@1/12	10.9	18.0	23.5	28.2	59.1	50.6	53.9/55.0	28.2/29.0	50.9	34.6	39.2	62.5	69.5	53.3	50.3
LaCo@1/6	10.9	18.5	26.2	27.7	59.5	46.9	51.7/54.0	25.7/29.0	45.3	36.0	36.2	61.8	68.4	50.5	48.5
LaCo@1/4	10.8	19.3	29.3	27.4	59.3	55.9	63.8/65.0	33.6/34.0	55.2	35.7	37.7	64.7	69.2	55.2	53.1
LaCo@1/2	11.0	20.0	39.0	26.3	59.3	60.8	68.1/70.0	38.5/39.0	56.9	36.4	37.5	65.5	70.6	54.2	54.9
LaCo@1	11.7	25.8	58.0	24.0	60.9	63.2	73.5/74.0	39.6/39.0	55.6	35.1	38.6	66.4	70.7	56.1	56.0
<i>One-Vision Training Setting</i>															
LaCo@1/12	10.9	13.4	23.0	28.1	61.0	53.4	51.6/53.0	29.0/29.0	54.9	36.0	37.5	65.7	65.9	53.9	51.0
LaCo@1/6	10.9	13.7	26.6	27.5	60.6	51.7	51.8/54.0	28.1/29.0	54.3	35.1	37.1	64.4	65.2	48.5	49.8
LaCo@1/4	10.8	13.9	29.5	27.6	61.8	59.2	62.4/64.0	34.7/34.0	58.7	35.2	39.5	62.0	66.7	55.4	53.6
LaCo@1/2	11.0	14.5	38.9	26.5	61.8	62.0	67.0/68.0	38.9/39.0	60.1	35.8	39.1	67.6	66.9	55.0	55.5
LaCo@1	11.7	18.9	57.6	24.0	62.2	65.6	71.8/73.0	40.1/41.0	60.1	36.2	40.9	67.9	64.3	54.2	56.4

Table 8: Performance and efficiency comparison between LaCo@1/12, LaCo@1/6, LaCo@1/4, LaCo@1/2 and LaCo@1 on single-image benchmarks.

Method	IEI	MI-VQA	NL-VR2	Puzzle	Q-Bench	Spot-Diff	TR-VQA	VST	3D-Chat	3D-TD	ScanQA	ALFRED	nuScenes	BLINK	Mantis	MathVerse	MuirBench	SciVerse	Avg.
	in-domain multi-image								in-domain multi-view				out-domain						
LaCo@1/12	30.0	79.7	73.4	44.0	49.0	38.0	60.3	30.6	60.8	49.0	30.4	56.5	70.0	39.7	45.8	34.6	31.0	35.1	47.7
LaCo@1/6	29.4	87.3	72.7	35.9	48.4	39.3	61.5	30.9	60.5	48.9	30.0	60.1	68.2	41.3	43.9	35.5	31.4	31.8	47.6
LaCo@1/4	30.0	85.0	73.2	43.9	48.5	38.8	60.5	30.6	60.5	48.9	30.3	59.7	72.5	41.3	44.4	34.3	31.9	30.4	48.0
LaCo@1/2	29.9	84.8	76.1	43.6	48.1	36.4	65.0	30.1	60.7	48.9	31.3	59.2	75.0	41.2	45.8	32.6	31.7	40.0	48.9
LaCo@1	30.4	82.8	75.7	42.4	49.9	37.3	66.1	30.2	60.6	49.1	31.3	59.5	73.0	40.5	44.9	42.5	35.9	41.8	49.7

Table 9: Performance and efficiency comparison between LaCo@1/12, LaCo@1/6, LaCo@1/4, LaCo@1/2 and LaCo@1 on multi-image benchmarks.